Received: 5 November 2018 | Revised: 1 March 2019 | Accepted: 15 March 2019

DOI: 10.1002/aic.16602

PROCESS SYSTEMS ENGINEERING

AIChE JOURNAL

Linear method for the design of shell and tube heat exchangers using the Bell–Delaware method

Caroline de O. Gonçalves[1] | André L. H. Costa[2] | Miguel J. Bagajewicz[3]

[1]School of Science and Technology, Unigranrio University, Duque de Caxias, Rio de Janeiro, Brazil

[2]Institute of Chemistry, Rio de Janeiro State University (UERJ), Rio de Janeiro, Rio de Janeiro, Brazil

[3]School of Chemical, Biological and Materials Engineering, University of Oklahoma, Norman, Oklahoma

Correspondence
André L. H. Costa, Institute of Chemistry, Rio de Janeiro State University (UERJ), Rua São Francisco Xavier, 524, Maracanã, Rio de Janeiro, RJ, CEP 20550-900 Brazil.
Email: andrehc@uerj.br

Funding information
Conselho Nacional de Desenvolvimento Científico e Tecnológico, Grant/Award Number: Process 311225/2016-0; Fundação Carlos Chagas Filho de Amparo à Pesquisa do Estado do Rio de Janeiro; Universidade do Estado do Rio de Janeiro, Grant/Award Number: Programa Prociência; National Council for Scientific and Technological Development

Abstract

In this article, we present a rigorous reformulation of the Bell–Delaware model for the design optimization of shell and tube heat exchanger to obtain a linear model. We extend a previously presented methodology1,2 of rigorously reformulate the mixed-integer nonlinear programing Kern model and we add disjunctions to automatically choose the different correlations to calculate heat transfer coefficients and pressure drop under different flow regimes. The linear character of the formulation allows the identification of the global optimum, even using conventional optimization algorithms. The proposed mixed-integer linear programming formulation with the Bell–Delaware method is able to identify feasible solutions for the design of heat exchangers at a lower cost than those obtained through conventional design formulations in the literature. Comparisons with the Kern method also indicate an average 22% difference (usually lower) in area.

KEYWORDS
design (process simulation), optimization

1 | INTRODUCTION

The traditional approach for the design of shell-and-tube heat exchangers involves a trial-and-verification procedure, where for each solution candidate, a skilled engineer must identify the constraint violations (e.g., shell-side pressure-drop higher than the allowable value) and propose modifications to attain a feasible solution (e.g., increase the baffle spacing or other changes).[1] Because this procedure usually stops when a feasible exchanger is obtained as often recommended, the resulting solution is not necessarily optimal and usually depends on the initial choices. Contrasting, optimization tools have also been proposed, where the objective function is the heat exchanger area for a given set of allowable pressure drops or the total annualized cost, encompassing capital and operating costs.[2] There are also multiobjective approaches.[3]

Design procedures based on heuristic methods search for the optimal solution employing graphical[4] or screening algorithms[5] associated to the thermofluid dynamic model of the equipment. Metaheuristic methods employ randomized search algorithms associated to a rating routine that provides the performance of each visited solution candidate (simulated annealing,[6] genetic algorithms,[7,8] particle swarm optimization,[9] artificial bee colony,[10] firefly algorithm,[11] etc.). Their performance was compared in several papers[12–14] and their hybridization with mathematical programming was also explored.[15]

Among different alternatives using mathematical programming, Jegede and Polley[2] presented a nonlinear programming model where the independent variables are the tube-side and shell-side heat transfer coefficients (or a convective heath transfer coefficient and the area). In turn, Mizutani et al.,[16] Ravagnani and Caballero,[17] and Onishi et al.[18] considered some optimization variables to be discrete, which yielded nonconvex mixed-integer nonlinear programing (MINLP) problems. In addition, Gonçalves et al.[19] showed that the nonlinear equations of the heat exchanger model based on the Kern method can be reformulated as a mixed-integer linear programming problem (MILP), whose solution is

therefore global. They also proposed a more efficient integer linear programming problem formulation.[20]

Due to the complexity of the shell-side flow, a key-issue in the heat exchanger modeling is the corresponding thermofluid dynamic modeling.[21] The stream analysis method[22] is considered to be the most accurate model employed in heat exchanger design, but because the details are proprietary, the methods of Kern[23] and Bell–Delaware[24,25] are still popular. The Bell–Delaware method is more accurate than Kern method, because it explicitly accounts for the influence of each individual by-pass and leakage streams in the shell-side.

The central aspect in this article is to show that the mathematical techniques developed by Gonçalves et al.[19,20] to transform nonlinear (and nonconvex) equipment models to linear ones can also be employed when several disjunctions for laminar and turbulent flow for tube-side and shell-side flows are needed (e.g., as it occurs in the Bell–Delaware method).

2 | NONLINEAR HEAT EXCHANGER DESIGN MODEL

We consider single E-type shell, single phase on both sides, single segmental baffles uniformly distributed without sealing strips and several tube passes, fixed fouling factors and we ignore pressure drops in the nozzles and the tube lane partition bypass stream. Eight design variables characterize each candidate solution: number of passes on the tube-side (*Npt*), tube diameter (outer and inner: *dte* and *dti*), tube layout (*lay*), tube pitch ratio (*rp*), number of baffles (*Nb*), shell diameter (*Ds*), tube length (*L*), and baffle cut ratio (*Bc*). The tube pitch ratio is the ratio between the tube pitch and the outer tube diameter. The baffle cut ratio is the ratio between the baffle cut and the inner shell diameter. We show model parameters using the symbol "ˆ" on the top. The discrete nature of the design variables is represented by the following generic constraints for *dte*.

$$dte = \sum_{sd=1}^{sdmax} \widehat{pdte}_{sd}\, yd_{sd} \tag{1}$$

$$\sum_{sd=1}^{sdmax} yd_{sd} = 1 \tag{2}$$

The rest of the discrete variables are *dti*, *Ds*, *lay*, *Npt*, *rp*, *L*, *Nb*, and *Bc*. The corresponding parameters are $\widehat{pdti}_{sd}$, $\widehat{pDs}_{sDs}$, $\widehat{play}_{slay}$, $\widehat{pNpt}_{sNpt}$, $\widehat{prp}_{srp}$, $\widehat{pL}_{sL}$, $\widehat{pNb}_{sNb}$, and $\widehat{pBc}_{sBc}$, respectively. The set of constraints is accompanied by a summation of binaries (yDs_{sDs}, $ylay_{slay}$, $yNpt_{sNpt}$, yrp_{srp}, yL_{sL}, yNb_{sNb}, *and* yBc_{sBc}) equal to 1 so that only one option is chosen.

The clearances and diameters are illustrated by Figure 1: *Dctl* is the diameter of the circle delimited by the centers of the outer tubes of the bundle, and *Dotl* is the tube bundle diameter. They are related to other variables by:

$$Dctl = Ds - Lbb - dte \tag{3}$$

$$Dotl = Ds - Lbb \tag{4}$$

where *Lbb* is the diametral clearance between the shell and the tube bundle. Two angles associated to the model are also defined: θDs is the central angle defined by the intercession of the baffle cut edge with the shell and θctl is the central angle delimited by the intercession between the baffle cut edge and the circle associated to the centers of the outer tubes. They are related to other variables as follows:

$$\theta Ds = 2\arccos[1-(2Bc)] \tag{5}$$

$$\theta ctl = 2\arccos\left\{\frac{Ds}{Dctl}[1-(2\,Bc)]\right\} \tag{6}$$

The total number of tubes in a given shell (*Ntt*) and their relation to diameters and other variables are available in tube count tables

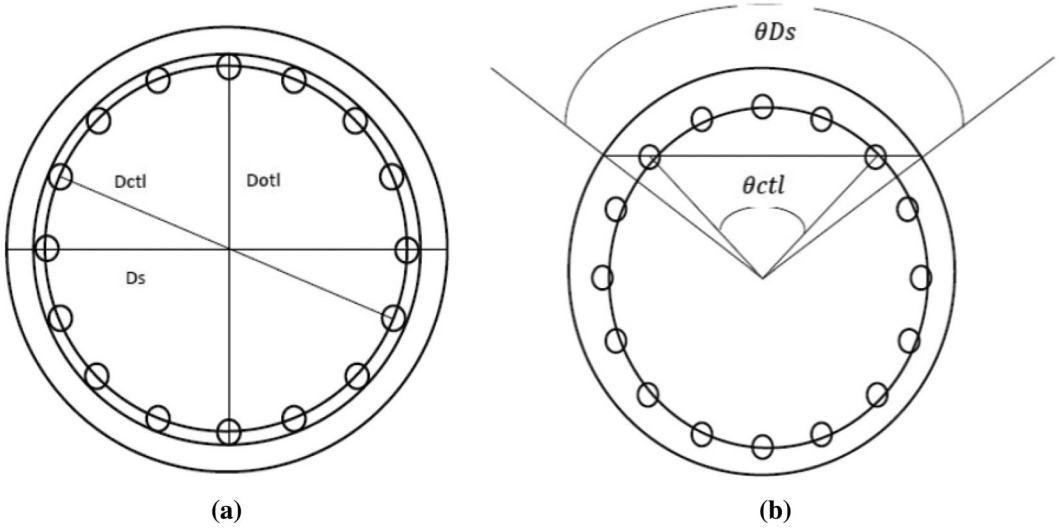

FIGURE 1 Geometry for (a) diameters *Dctl*, *Dotl*, and *Ds* and (b) angles θDs and θctl

with mathematical equations and algorithms for its evaluation.[26] In this article, we use a set of equations from Taborek,[27] organized as mathematical constraints of the optimization problem, as follows:

$$Ntt = \frac{0.78 Dctl^2}{C1\, ltp^2}(1-\psi_n) \tag{7}$$

The parameter $C1$ is equal to 0.866 for a 30° layout or 1.00 for 45° and 90° layouts. Therefore:

$$C1 = 0.866 ylay_1 + 1.00(ylay_2 + ylay_3) \tag{8}$$

The correction factor ψ_n represents the omission of tubes inside the shell due to the presence of multiple tube passes. Based on a graph published by Taborek,[27] this parameter can be represented by a set of values, which depends on the number of tube passes and the shell diameter (for the sake of simplification the dependence on the tube diameter was dismissed):

$$\psi_n = \sum_{sNpt=1}^{sNptmax} \sum_{sDs=1}^{sDsmax} \left(\widehat{P\psi_n}\right)_{sNpt,sDs} yNpt_{sNpt} yDs_{sDs} \tag{9}$$

where the values of the parameter $\left(\widehat{P\psi_n}\right)_{sNpt,sDs}$ are displayed in the Supporting Information.

Next, *Ntcc* is the number of tube rows crossed between baffle tips and *Ntcw* is the effective number of tube rows crossed in the baffle window:

$$Ntcc = \frac{Ds}{Lpp}[1-(2\,Bc)] \tag{10}$$

$$Ntcw = \frac{0.8}{Lpp}\left[(Ds\,Bc) - \frac{(Ds-Dctl)}{2}\right] \tag{11}$$

where *Lpp* is equal to 0.866*ltp* for 30° layout (*slay* = 1), *ltp* for 90° layout (*slay* = 2), and 0.707*ltp* for 45° layout (*slay* = 3). This relation is represented by:

$$Lpp = 0.866\, ltp\, ylay_1 + ltp\, ylay_2 + 0.707\, ltp\, ylay_3 \tag{12}$$

The total number of rows crossed along the entire heat exchanger (*Nc*) is given by:

$$Nc = (Ntcc + Ntcw)(Nb+1) \tag{13}$$

where *Nb* is the number of baffles. For a uniform distribution of the baffles along the tube length, the relation between the baffle spacing (*lbc*) and the number of baffles is:

$$Nb = L/lbc - 1 \tag{14}$$

The fraction of the number of tubes inside one window (*Fw*) is:

$$Fw = \frac{\theta ctl - \sin\theta ctl}{2\pi} \tag{15}$$

Then, the fraction of the number of tubes in pure cross flow between baffle tips (*Fc*) is:

$$Fc = 1 - 2Fw \tag{16}$$

The cross-flow area is delimited between adjacent baffles, evaluated at the shell center:

$$Sm = lbc\left[Lbb + \frac{Dctl}{ltp_{eff}}(ltp - dte)\right] \tag{17}$$

where *ltp* is the tube pitch, and ltp_{eff} is the distance between tubes along the rows perpendicular to the flow. The value of ltp_{eff} depends on the tube layout, it is equal to *ltp* for 30° and 90° layouts and it is equal to 0.707*ltp* for 45° layout:

$$ltp_{eff} = ltp(ylay_1 + ylay_2 + 0.707\, ylay_3) \tag{18}$$

According to the definition of the tube pitch ratio:

$$ltp = rp\, dte \tag{19}$$

The flow through the baffle window is associated to the free flow area in that region (*Sw*), that is calculated by the difference between the gross window flow area (*Swg*), that is, excluding the presence of the tubes, and the area occupied by the tubes (*Swt*):

$$Sw = Swg - Swt \tag{20}$$

$$Swg = \frac{\pi}{4}Ds^2\left(\frac{\theta Ds - \sin\theta Ds}{2\pi}\right) \tag{21}$$

$$Swt = Ntw\left(\frac{\pi}{4}dte^2\right) \tag{22}$$

where *Ntw* is the number of tubes in the window, which is equivalent by the total number of tubes (*Ntt*) multiplied by the fraction of the number of tubes in one window (*Fw*):

$$Ntw = Ntt\, Fw \tag{23}$$

The flow area between the shell and the baffle (*Ssb*) is:

$$Ssb = \pi Ds\left(\frac{Lsb}{2}\right)\left(1 - \frac{\theta Ds}{2\pi}\right) \tag{24}$$

where *Lsb* is the shell-to-baffle diametral clearance.

The area of the flow through the hole leakage area of the baffle (*Stb*) is:

$$Stb = Ntt(1-Fw)\left\{\frac{\pi}{4}\left[(dte + Ltb)^2 - dte^2\right]\right\} \tag{25}$$

where *Ltb* is the tube-to-baffle clearance. The bypass flow area between the tube bundle and the shell is given by:

$$Sb = lbc[(Ds - Dotl) + Lpl] \tag{26}$$

where *Lpl* expresses the effect of the tube lane partition bypass width (in the proposed model, this gap was dismissed, then *Lpl* = 0).

The model also contains factors related to the area ratios: *rs* is the ratio of the shell-to-baffle leakage area to the sum of this area and the tube-to-baffle leakage area, *rlm* is the ratio of both leakage areas to the cross-flow area, *Fsbp* is the ratio of the bypass area between the tube bundle and the shell to the cross-flow area:

$$rs = \frac{Ssb}{Ssb + Stb} \tag{27}$$

$$rlm = \frac{Ssb + Stb}{Sm} \tag{28}$$

$$Fsbp = \frac{Sb}{Sm} \tag{29}$$

Expressions for evaluation of the clearances *Lbb* (for fixed tubesheet or U tubes) and *Lsb* (based on TEMA standards[28]) are given by Taborek,[27] respectively:

$$Lbb = 12.8 \cdot 10^{-3} + 4.8 \cdot 10^{-3} Ds \tag{30}$$

$$Lsb = 3.1 \cdot 10^{-3} + 4 \cdot 10^{-3} Ds \tag{31}$$

The diametral clearance between the outer tube diameter and the baffle hole is also established by TEMA standards, as follows:

$$dte > 0.03175\,\text{m} \rightarrow Ltb = 0.008\,\text{m} \tag{32}$$

$$dte \le 0.03175\,\text{m and } lbmax \le 0.900\,\text{m} \rightarrow Ltb = 0.008\,\text{m} \tag{33}$$

$$dte \le 0.03175\,\text{m and } lbmax > 0.900\,\text{m} \rightarrow Ltb = 0.004\,\text{m} \tag{34}$$

where *lbmax* is the maximum unsupported span of the tubes, calculated according to TEMA recommended values (see Equation (93)). In the optimization problem, the relations related to Equations (32)–(34) are represented by a set of values that can be calculated previously depending on the design alternatives:

$$Ltb = \sum_{sd=1}^{sdmax} \sum_{sL=1}^{sLmax} \sum_{sNb=1}^{sNbmax} \widehat{pLtb}_{sDs,sL,sNb}\, yd_{sd}\, yL_{sL}\, yNb_{sNb} \tag{35}$$

2.1 | Shell-side thermal and hydraulic equations

There are some slightly different variations in the literature of the Bell–Delaware method.[22] We employ equations based on Taborek.[27]

The heat transfer coefficient is calculated using the Reynolds ($Res = dte\, Gs/\widehat{\mu s}$) and Prandtl numbers ($\widehat{Prs} = \widehat{Cps}\,\widehat{\mu s}/\widehat{ks}$) for the shell-side stream, associated to the mass flux $Gs = \widehat{ms}/Sm$.The shell-side heat transfer coefficient corresponds to the ideal tube bank coefficient (*hi*) multiplied by a series of factor that accounts the by-pass and leakage streams:

$$hs = hi(Jc\, Jl\, Jb\, Jr) \tag{36}$$

where *Jc* is the segmental baffle window correction factor, *Jl* is the correction factor for baffle leakage effects, *Jb* is the correction factor for bundle to shell bypass effects, *Jr* is the correction factor for adverse temperature gradient in laminar flow. The original Bell–Delaware method also uses a correction factor for unequal baffle spacing at the inlet or outlet (we do not include it here; we use uniform distribution of the baffle spacing). In turn, the shell-side heat transfer coefficient for ideal tube bank is given by:

$$hi = ji\, \widehat{Cps}\, Gs\, \widehat{Prs}^{-2/3} \tag{37}$$

where *ji* is the Colburn's heat transfer factor for ideal tube bank flow:

$$ji = a1\left(\frac{1.33}{rp}\right)^{a} Res^{a2} \tag{38}$$

The parameters *a*, *a*1, *a*2, and *a*3 are given by:

$$a = \frac{a3}{1 + 0.14 Res^{a4}} \tag{39}$$

$$a1 = \sum_{sRes=1}^{sResmax} \sum_{slay=1}^{slaymax} \widehat{Pa1}_{sRes,slay}\, yRes_{sRes}\, ylay_{slay} \tag{40}$$

$$a2 = \sum_{sRes=1}^{sResmax} \sum_{slay=1}^{slaymax} \widehat{Pa2}_{sRes,slay}\, yRes_{sRes}\, ylay_{slay} \tag{41}$$

$$a3 = \sum_{sRes=1}^{sResmax} \sum_{slay=1}^{slaymax} \widehat{Pa3}_{sRes,slay}\, yRes_{sRes}\, ylay_{slay} \tag{42}$$

$$a4 = \sum_{sRes=1}^{sResmax} \sum_{slay=1}^{slaymax} \widehat{Pa4}_{sRes,slay}\, yRes_{sRes}\, ylay_{slay} \tag{43}$$

where the values of the parameters $\widehat{Pa1}_{sRes,slay}$, $\widehat{Pa2}_{sRes,slay}$, $\widehat{Pa3}_{sRes,slay}$, and $\widehat{Pa4}_{sRes,slay}$ are displayed in the Supporting Information.

The binary variables $yRes_{sRes}$ allow the regime choice through:

$$Res \le 10 yRes_1 + 20 yRes_2 + 10^2 yRes_3 + 10^3 yRes_4 + 10^4 yRes_5 + 10^5 yRes_6 \tag{44}$$

$$Res \ge 10 yRes_2 + 20 yRes_3 + 10^2 yRes_4 + 10^3 yRes_5 + 10^4 yRes_6 + \hat{\varepsilon} \tag{45}$$

$$\sum_{sRes=1}^{sResmax} yRes_{sRes} = 1 \tag{46}$$

where $\hat{\varepsilon}$ is a small positive number and it is required to the correct identification of the different ranges.

The correction factors that contribute to calculate *hs* are given by:

$$Jc = 0.55 + 0.72Fc \tag{47}$$

$$Jl = 0.44(1-rs) + [1-0.44(1-rs)]\exp(-2.2rlm) \tag{48}$$

$$Jb = \exp[-Cbh\,Fsbp] \tag{49}$$

$$Jr = Jr1\,(yRes_1 + yRes_2) + Jr2\,yRes_3 + Jr3\,(yRes_4 + yRes_5 + yRes_6) \tag{50}$$

where *Cbh* is equal to 1.35 for laminar flow (Res ≤ 100) and 1.25 for turbulent and transition flow (Res > 100), thus *Cbh* corresponds to:

$$Cbh = 1.35(yRes_1 + yRes_2 + yRes_3) + 1.25(yRes_4 + yRes_5 + yRes_6) \tag{51}$$

The heat transfer correction factors for adverse temperature gradient in laminar flow are:

$$Jr1 = \left(\frac{10}{Nc}\right)^{0.18} \text{ for } Res \le 20 \tag{52}$$

$$Jr2 = Jr1 + \left(\frac{20-Res}{80}\right)[Jr1-1] \text{ for } 20 < Res \le 100 \tag{53}$$

$$Jr3 = 1 \text{ for } Res > 100 \tag{54}$$

The shell-side pressure drop (ΔPs) includes the pressure drop in the flow through the tube bundle between adjacent baffles in cross flow (ΔPc), the pressure drop in the baffle windows (ΔPw), and the pressure drop at the end zones (ΔPe):

$$\Delta Ps = \Delta Pc + \Delta Pw + \Delta Pe \tag{55}$$

In turn, the pressure drop of the cross flow between baffle tips is given by:

$$\Delta Pc = \Delta Pbi\,(Nb-1)\,Rb\,Rl \tag{56}$$

where ΔPbi is the ideal bank pressure drop delimited by one central baffle spacing, *Rb* is the by-pass correction factor, and *Rl* is the leakage correction factor. Finally, the ideal bank pressure drop between baffle tips is given by:

$$\Delta Pbi = 2\,fs\,Ntcc\frac{Gs^2}{\hat{\rho}s} \tag{57}$$

where *fs* is the friction factor for ideal tube bank flow, given by:

$$fs = b1\left(\frac{1.33}{rp}\right)^b Res^{b2} \tag{58}$$

The values of *b*, *b*1, *b*2, *b*3, and *b*4 are represented by the following expressions:

$$b = \frac{b3}{1+0.14Res^{b4}} \tag{59}$$

$$b1 = \sum_{sRes=1}^{sResmax}\sum_{slay=1}^{slaymax} \widehat{Pb1}_{sRes,slay}\,yRes_{sRes}\,ylay_{slay} \tag{60}$$

$$b2 = \sum_{sRes=1}^{sResmax}\sum_{slay=1}^{slaymax} \widehat{Pb2}_{sRes,slay}\,yRes_{sRes}\,ylay_{slay} \tag{61}$$

$$b3 = \sum_{sRes=1}^{sResmax}\sum_{slay=1}^{slaymax} \widehat{Pb3}_{sRes,slay}\,yRes_{sRes}\,ylay_{slay} \tag{62}$$

$$b4 = \sum_{sRes=1}^{sResmax}\sum_{slay=1}^{slaymax} \widehat{Pb4}_{sRes,slay}\,yRes_{sRes}\,ylay_{slay} \tag{63}$$

where the values of the parameters $\widehat{Pb1}_{sRes,slay}$, $\widehat{Pb2}_{sRes,slay}$, $\widehat{Pb3}_{sRes,slay}$, and $\widehat{Pb4}_{sRes,slay}$ are displayed in the Supporting Information.

The correction factor *Rb*, considering no sealing strips, is given by:

$$Rb = \exp[-Cbp\,Fsbp] \tag{64}$$

where *Cbp* is equal to 4.5 for laminar flow and is equal to 3.7 for transition and turbulent flow and, for the optimization problem, is expressed by:

$$Cbp = 4.5(yRes_1 + yRes_2 + yRes_3) + 3.7\,(yRes_4 + yRes_5 + yRes_6) \tag{65}$$

The correction factor *Rl* is given by:

$$Rl = \exp\left[-1.33(1+rs)(rlm)^p\right] \tag{66}$$

$$p = -0.15(1+rs) + 0.8 \tag{67}$$

The pressure drop in the baffle windows depends on the mass flux in relation to the geometric mean of the cross-flow area and the window area ($Gw = \widehat{ms}/\sqrt{SmSw}$). Therefore, the pressure drop expression (*Res* < 100) for laminar flow is equal to:

$$\Delta Pw^{lam} = Nb\,Rl\left\{26\frac{Gw\,\widehat{\mu s}}{\hat{\rho}s}\left[\frac{Ntcw}{Ltp-dte}+\frac{lbc}{Dw^2}\right]+\left[2\frac{Gw^2}{\hat{\rho}s}\right]\right\} \tag{68}$$

where the hydraulic diameter (*Dw*) is equal to:

$$Dw = \frac{4\,Sw}{\pi\,dte\,Ntw + \pi\,Ds\left(\frac{\theta Ds}{2\pi}\right)} \tag{69}$$

The corresponding expression for turbulent flow (*Res* ≥ 100) is:

$$\Delta Pw^{turb} = Nb\,Rl\left[(2+0.6Ntcw)\frac{Gw^2}{2\hat{\rho}s}\right] \tag{70}$$

Thus, the pressure drop in the baffle windows for the optimization problem is:

$$\Delta Pw = \Delta Pw^{lam}(yRes_1 + yRes_2 + yRes_3) + \Delta Pw^{turb}(yRes_4 + yRes_5 + yRes_6) \tag{71}$$

The pressure drop at both end zones is equal to:

$$\Delta Pe = \Delta Pbi\left(1+\frac{Ntcw}{Ntcc}\right)Rb\,Rs \tag{72}$$

where Rs is the end zone correction factor:

$$Rs = \left(\frac{lbc}{lbo}\right)^{2-n} + \left(\frac{lbc}{lbi}\right)^{2-n} \tag{73}$$

where $n = 1$ for laminar ($Res < 100$) and $n = 0.2$ for turbulent ($Res \geq 100$). However, according to the assumption that all baffle spacings are equal, this expression becomes equal to 2.

2.2 | Tube-side thermal and hydraulic equations

The Reynolds ($Ret = dti\,vt\,\widehat{\rho t}/\widehat{\mu t}$) and Prandtl numbers ($\widehat{Prt} = \widehat{Cpt}\,\widehat{\mu t}/\widehat{kt}$) of the tube-side flow compose the heat transfer correlations for the determination of the Nusselt number ($Nut = ht\,dti/\widehat{kt}$), where $\widehat{\rho t}$ is the density, $\widehat{Cpt}$ is the heat capacity, $\widehat{\mu t}$ is the viscosity, and $\widehat{kt}$ is the thermal conductivity. The flow velocity is given by:

$$vt = \frac{4\,\widehat{mt}}{Ntp\,\pi\,\widehat{\rho t}\,dti^2} \tag{74}$$

where $\widehat{mt}$ is the mass flow rate and Ntp is the number of tubes per pass (calculated by the ratio between the total number of tubes, Ntt, and the number of passes in the tubes, Npt).

The adopted modeling for the evaluation of the convective heat transfer coefficient in the tube-side contemplates laminar, transitional, and turbulent flow according to the proposal of Incropera and De Witt.[29] The evaluation of the Nusselt number for the turbulent and transition regimes employs the Gnielinski correlation ($2{,}300 < Ret < 5{\cdot}10^6$):

$$Nut^{Gni} = \frac{(ft/8)(Ret-1000)\widehat{Prt}}{1+12.7(ft/8)^{1/2}\left(\widehat{Pr}^{2/3}-1\right)} \tag{75}$$

where ft is tube-side Darcy friction factor. For the laminar flow ($Ret \leq 2{,}300$), the effects related to the entry region may be relevant. Therefore for $\widehat{Prt} > 5$, the Hausen correlation is employed:

$$Nut^{Hau} = 3.66 + \frac{0.0668(dti/L)\,Ret\,\widehat{Prt}}{1+0.04\left[(dti/L)\,Ret\,\widehat{Prt}\right]^{2/3}} \tag{76}$$

For $0.6 \leq \widehat{Prt} \leq 5$, the calculation of the Nusselt number employs the Sieder and Tate correlation:

$$Nut^{S\&T} = 1.86\left(\frac{Ret\widehat{Prt}}{L/dti}\right)^{1/3} \tag{77}$$

However, when the Nusselt falls lower than 3.66 (theoretical result for fully developed flow), then this limit value is used ($Nut^{theo} = 3.66$).

The head loss in the tube-side flow is[1]:

$$\Delta Pt = \widehat{\rho t}\,ft\frac{L}{dti}\frac{Npt\,vt^2}{2} + \frac{\widehat{\rho t}\,K\,Npt\,vt^2}{2} \tag{78}$$

where the parameter K, associated with the head loss in the heads, is equal to 0.9 for one tube pass and 1.6 for multiple passes. Considering all flow regimes, the friction factor is given by[1]:

$$ft^{lam} = \frac{64}{Ret} \text{ for } Ret \leq 1311 \tag{79}$$

$$ft^{trans} = 0.0488 \text{ for } 1{,}311 < Ret < 3{,}380 \tag{80}$$

$$ft^{turb} = 0.014 + \frac{1.056}{\mathrm{Re}t^{0.42}} \text{ for } Ret \geq 3{,}380 \tag{81}$$

The evaluation of the Nusselt number and the friction factor associated to the selection of the proper regime can be expressed using binary variables:

$$\begin{aligned} Nut = {} & Nut^{theo}(yRet_1 + yRet_2)\,yNut_1 + Nut^{S\&T}(yRet_1 + yRet_2)\,\widehat{PyPrt}\,yNut_2 \\ & + Nut^{Hau}(yRet_1 + yRet_2)\left(1-\widehat{PyPrt}_1\right)yNut_2 \\ & + Nut^{Gni}(yRet_3 + yRet_4) \end{aligned} \tag{82}$$

$$ft = ft^{lam}yRet_1 + ft^{trans}(yRet_2 + yRet_3) + ft^{turb}yRet_4 \tag{83}$$

where the parameter $\widehat{PyPrt}$ is equal to 1 if $\widehat{Prt} \leq 5$, otherwise it is zero. The ranges of the Reynolds number associated to the binary variables are: <1,311 ($sRet = 1$), 1,311 to 2,300 ($sRet = 2$), 2,300 to 3,380 ($sRet = 3$), and >3,380 ($sRet = 4$). Thus,

$$Ret \leq 1{,}311yRet_1 + 2{,}300yRet_2 + 3{,}380yRet_3 + \widehat{URet}yRet_4 \tag{84}$$

$$Ret \geq 1{,}311yRet_2 + 2{,}300yRet_3 + 3{,}380yRet_4 + \hat{\varepsilon} \tag{85}$$

$$\sum_{sRet=1}^{sRetmax} yRet_{sRet} = 1 \tag{86}$$

$$Nut < 3.66\, yNut_1 + \widehat{UNut}\, yNut_2 \tag{87}$$

$$Nut \geq 3.66\, yNut_2 + \hat{\varepsilon} \tag{88}$$

where $\hat{\varepsilon}$ is a small positive number. The parameter $\widehat{URet} = 5{\cdot}10^6$ is an upper bond on the Reynolds number, consistent with the validity range of the Gnielinski correlation. The upper bound parameter $\widehat{UNut}$ is assumed equal to $4{\cdot}10,^2$ calculated accordingly the value of $\widehat{URet}$.

2.3 | Heat transfer rate equation and overall heat transfer coefficient

For the area equation, we use a design margin ("excess area", $\widehat{Aexc}$):

$$UA \geq \left(1 + \frac{\widehat{Aexc}}{100}\right) \frac{\hat{Q}}{\widehat{\Delta Tlm}\, F} \tag{89}$$

The overall heat transfer coefficient is:

$$U = \frac{1}{\frac{dte}{dti\, ht} + \frac{\widehat{Rft}\, dte}{dti} + \frac{dte \ln\left(\frac{dte}{dti}\right)}{\widehat{2\, ktube}} + \widehat{Rfs} + \frac{1}{hs}} \tag{90}$$

The area of the heat exchanger is the sum of the area of each individual tube:

$$A = Ntt\pi\, dte\, L \tag{91}$$

where $\widehat{ktube}$ is the thermal conductivity of the tube wall, and $\widehat{Rft}$ and $\widehat{Rfs}$ are the tube-side and shell-side fouling factors. The LMTD correction factor is 1 for countercurrent flow and, for an even number of tube passes, depends on the end temperatures ($\widehat{Fmp}$) (see Supporting Information for the corresponding expression):

$$F = 1\, yNpt_1 + \widehat{Fmp} \sum_{sNpt=2}^{sNptmax} yNpt_{sNpt} \tag{92}$$

2.4 | Bounds on pressure drops, flow velocities, and geometric constraints

Lower and upper bounds constraints on pressure drops and flow velocities are added and because design recommendations impose that the baffle spacing must be between 20 and 100% of the shell diameter[27] we use $lbc \geq 0.2\, Ds$ and $lbc \leq 1.0\, Ds$.

We use TEMA standards upper bound on the maximum unsupported span of the tubes (*lbmax*), which prevents sagging and vibration, is dependent on the nature of the material and the outer tube diameter[28]:

$$lbmax = \widehat{plbmax}1\, dte + \widehat{plbmax}2 \tag{93}$$

where, for tube diameters higher than 19 mm (3/4 in), $\widehat{plbmax}1 = 52$ and $\widehat{plbmax}2 = 0.532$ m for steel and steel alloys, and $\widehat{plbmax}1 = 46$ and $\widehat{plbmax}2 = 0.436$ m, for aluminum and copper alloys.

The maximum unsupported span is related to the window region, then the constraint involving the baffle spacing is $lbc \leq lbmax/2$. Finally, the ratio between exchanger length and shell diameter must be between 3 and 5 ($L \geq 3\, Ds$ and $L \leq 15\, Ds$).[27]

2.5 | Objective function

Two alternative objective functions are considered to be minimized. The first objective function is the area associated to given values of maximum pressure drops, and the second objective function is the total annualized cost (capital and operating costs in a yearly basis). According to Mizutani et al.,[16] this alternative of objective function can be represented by:

$$\widehat{a_{cost}} A^{\widehat{b_{cost}}} + P_{cost} \tag{94}$$

where $\widehat{a_{cost}}$ and $\widehat{b_{cost}}$ are parameters for the evaluation of the annualized capital cost of the heat exchanger and P_{cost} is the pumping cost:

$$P_{cost} = \widehat{c_{cost}} \left(\frac{\Delta Pt\, \widehat{mt}}{\widehat{\rho t}} + \frac{\Delta Ps\, \widehat{ms}}{\widehat{\rho s}}\right) \tag{95}$$

3 | DEVELOPMENT OF THE MILP FORMULATION

To obtain an MILP formulation, we use the relations between the discrete variables and the corresponding binary variables as in previous work.[20,30] Instead of representing each discrete alternative of each variable by an individual index, a single index, *srow*, is associated to each set of discrete values which compose a candidate solution. Therefore, a binary variable $yrow_{srow}$ expresses the relation between the discrete variables and the corresponding binary variables. For example, for *dte*, it is

$$dte = \sum_{srow} \widehat{Pdte}_{srow}\, yrow_{srow} \tag{96}$$

The rest of variables (*dti*, *Ds*, *lay*, *Npt*, *rp*, *L*, *Nb*, *and Bc*) are represented by similar equations using the following parameters $\widehat{Pdti}_{srow}$, $\widehat{PDs}_{srow}$, $\widehat{Play}_{srow}$, $\widehat{PNpt}_{srow}$, $\widehat{Prp}_{srow}$, $\widehat{PL}_{srow}$, $\widehat{PNb}_{srow}$, $\widehat{PBc}_{srow}$.

The next step consists of a reformulation.[20,30] Thus, an expression as

$$p^{n1} q^{n2} \cdots z^{nm} = \left[\sum_{srow} \widehat{pd}_{srow}\, yrow_{srow}\right]^{n1} \left[\sum_{srow} \widehat{qd}_{srow}\, yrow_{srow}\right]^{n2} \left[\sum_{srow} \widehat{zd}_{srow}\, yrow_{srow}\right]^{nm} \tag{97}$$

is reorganized to:

$$p^{n1} q^{n2} \cdots z^{nm} = \sum_{srow} \left(\widehat{pd}_{srow}\right)^{n1} \left(\widehat{qd}_{srow}\right)^{n2} \ldots\ldots \left(\widehat{zd}_{srow}\right)^{nm} yrow_{srow} \tag{98}$$

We then linearize products of binaries as in previous work.[20,30]

4 | MILP FORMULATION

This section presents the complete linear formulation of the optimal heat exchanger design problem resultant of the application of the techniques described above.

4.1 | Heat transfer rate equations

$$\hat{Q}\left[\sum_{srow}\frac{\widehat{Pdte}_{srow}}{\widehat{kt}}\left\{\frac{1}{\widehat{PNut1}}wyrowNut1Ret1_{srow}\right.\right.$$
$$+\frac{\widehat{PyPrt}}{\widehat{PNut2}_{srow}}wyrowNut2Ret1_{srow}+\frac{1-\widehat{PyPrt}}{\widehat{PNut3}_{srow}}wyrowNut2Ret1_{srow}$$
$$+\frac{1}{\widehat{PNut1}}wyrowNut1Ret2_{srow}+\frac{\widehat{PyPrt}}{\widehat{PNut2}_{srow}}wyrowNut2Ret2_{srow}$$
$$+\frac{1-\widehat{PyPrt}}{\widehat{PNut3}_{srow}}wyrowNut2Ret2_{srow}+\frac{1}{\widehat{PNut4}_{srow}}wyrowRet3_{srow}$$
$$\left.+\frac{1}{\widehat{PNut5}_{srow}}wyrowRet4_{srow}\right\}+\sum_{srow}\frac{\widehat{Rft}\,\widehat{Pdte}_{srow}}{\widehat{Pdti}_{srow}}yrow_{srow}$$
$$+\sum_{srow}\frac{\widehat{Pdte}_{srow}\ln\left(\frac{\widehat{Pdte}_{srow}}{\widehat{Pdti}_{srow}}\right)}{2\,\widehat{ktube}}yrow_{srow}+\widehat{Rfs}$$
$$\left.+\sum_{sRes=1}^{sResmax}\sum_{srow}\frac{1}{\widehat{Phs}_{srow,sRes}}wyrowRes_{srow,sRes}\right]\le$$
$$\sum_{srow}\pi\widehat{PNtt}_{srow}\widehat{Pdte}_{srow}\widehat{PL}_{srow}\left(\frac{100}{100+\widehat{Aexc}}\right)\widehat{\Delta Tlm}\left(\hat{F}_{srow}\right)yrow_{srow}) \quad (99)$$

where $\widehat{PNtt}_{srow}$ is the total number of tubes that can be calculated prior to the optimization using Equations (7)–(9). The expressions related to the other parameters are displayed in the Supporting Information.

4.2 | Binary variables

This constraint imposes that only one design alternative must be chosen:

$$\sum_{srow}yrow_{srow}=1 \quad (100)$$

The representation of the Reynolds number ranges are:

$$\sum_{sRet}yRet_{sRet}=1 \quad (101)$$

$$\sum_{sRes}yRes_{sRes}=1 \quad (102)$$

Similarly, for the Nusselt number in the tube-side:

$$yNut_1+yNut_2=1 \quad (103)$$

4.3 | Constraints relating continuous and binary variables

The linear constraints presented below depict the relations employed to eliminate the nonlinearities associated to the product of a continuous and a binary variable.

Product of the variables $yrow_{srow}$, $yNut_1$, and $yRet_1$:

$$wyrowNut1Ret1_{srow}\le yrow_{srow} \quad (104)$$

$$wyrowNut1Ret1_{srow}\le yNut_1 \quad (105)$$

$$wyrowNut1Ret1_{srow}\le yRet_1 \quad (106)$$

$$wyrowNut1Ret1_{srow}\ge yrow_{srow}+yNut_1+yRet_1-2 \quad (107)$$

Product of variables $yrow_{srow}$, $yNut_2$, and $yRet_1$:

$$wyrowNut2Ret1_{srow}\le yrow_{srow} \quad (108)$$

$$wyrowNut2Ret1_{srow}\le yNut_2 \quad (109)$$

$$wyrowNut2Ret1_{srow}\le yRet_1 \quad (110)$$

$$wyrowNut2Ret1_{srow}\ge yrow_{srow}+yNut_2+yRet_1-2 \quad (111)$$

Product of variables $yrow_{srow}$, $yNut_1$, and $yRet_2$:

$$wyrowNut1Ret2_{srow}\le yrow_{srow} \quad (112)$$

$$wyrowNut1Ret2_{srow}\le yNut_1 \quad (113)$$

$$wyrowNut1Ret2_{srow}\le yRet_2 \quad (114)$$

$$wyrowNut1Ret2_{srow}\ge yrow_{srow}+yNut_1+yRet_2-2 \quad (115)$$

Product of variables $yrow_{srow}$, $yNut_2$, and $yRet_2$:

$$wyrowNut2Ret2_{srow}\le yrow_{srow} \quad (116)$$

$$wyrowNut2Ret2_{srow}\le yNut_2 \quad (117)$$

$$wyrowNut2Ret2_{srow}\le yRet_2 \quad (118)$$

$$wyrowNut2Ret2_{srow}\ge yrow_{srow}+yNut_2+yRet_2-2 \quad (119)$$

Product of variables $yrow_{srow}$, and $yRet_3$:

$$wyrowRet3_{srow}\le yrow_{srow} \quad (120)$$

$$wyrowRet3_{srow}\le yRet_3 \quad (121)$$

$$wyrowRet3_{srow}\ge yrow_{srow}+yRet_3-1 \quad (122)$$

Product of variables $yrow_{srow}$, and $yRet_4$:

$$wyrowRet4_{srow} \le yrow_{srow} \tag{123}$$

$$wyrowRet4_{srow} \le yRet_4 \tag{124}$$

$$wyrowRet4_{srow} \ge yrow_{srow} + yRet_4 - 1 \tag{125}$$

Product of variables $yrow_{srow}$, and $yRet_{sRet}$:

$$wyrowRet_{srow,sRet} \le yrow_{srow} \tag{126}$$

$$wyrowRet_{srow,sRet} \le yRet_{sRet} \tag{127}$$

$$wyrowRet_{srow,sRet} \ge yrow_{srow} + yRet_{sRet} - 1 \tag{128}$$

Product of variables $yrow_{srow}$, and $yRes_{sRes}$:

$$wyrowRes_{srow,sRes} \le yrow_{srow} \tag{129}$$

$$wyrowRes_{srow,sRes} \le yRes_{sRes} \tag{130}$$

$$wyrowRes_{srow,sRes} \ge yrow_{srow} + yRes_{sRes} - 1 \tag{131}$$

4.4 | Constraints associated to the Reynolds and Nusselt numbers ranges

The formulation developed involving different flow regimes in the tube-side and in the shell-side yields the constraints represented below:

$$\sum_{srow} \widehat{PRes}_{srow} yrow_{srow} \le 10\, yRes_1 + 20\, yRes_2 + 10^2 yRes_3 + 10^3 yRes_4 + 10^4 yRes_5 + 10^5 yRes_6 \tag{132}$$

$$\sum_{srow} \widehat{PRes}_{srow} yrow_{srow} \ge 10\, yRes_2 + 20\, yRes_3 + 10^2 yRes_4 + 10^3 yRes_5 + 10^4 yRes_6 + \hat{\varepsilon} \tag{133}$$

$$\sum_{srow} \widehat{PRet}_{srow} yrow_{srow} \le 1,311\, yRet_1 + 2,300\, yRet_2 + 3,380\, yRet_3 + \widehat{URet}\, yRet_4 \tag{134}$$

$$\sum_{srow} \widehat{PRet}_{srow} yrow_{srow} \ge 1,311\, yRet_2 + 2,300\, yRet_3 + 3,380\, yRet_4 + \hat{\varepsilon} \tag{135}$$

$$\sum_{srow} \widehat{PNut2}_{srow} yrow_{srow} < 3.66\, yNut_1 + \widehat{UNut}\, yNut_2 \tag{136}$$

$$\sum_{srow} \widehat{PNut2}_{srow} yrow_{srow} \ge 3.66\, yNut_2 + \hat{\varepsilon} \tag{137}$$

4.5 | Bounds on pressure drops and flow velocities

The set of constraints presented below represents bounds on pressure drops and velocities. Instead to represent the velocity bounds in a conventional way, we have rewritten it based on an analysis of the search space, where it is possible to delimit the design alternatives that violate these constraints. Souza et al.[30] has concluded that this form of representation allow to reach a better computational performance.

Shell-side pressure upper bound:

$$\sum_{sRes=1}^{sResmax} \sum_{srow} P\Delta\widehat{Ps}_{srow,sRes}\, wyrowRes_{srow,sRes} \le \Delta\widehat{Psdisp} \tag{138}$$

where $P\Delta\widehat{Ps}_{srow,sRes} = P\Delta\widehat{Pc}_{srow,sRes} + P\Delta\widehat{Pw}_{srow,sRes} + P\Delta\widehat{Pe}_{srow,sRes}$.

Tube-side pressure upper bound:

$$\sum_{sRet=1}^{sRetmax} \sum_{srow} P\Delta\widehat{Pt}_{srow,sRet}\, wyrowRet_{srow,sRet} \le \Delta\widehat{Ptdisp} \tag{139}$$

where $P\Delta\widehat{Pt}_{srow,sRet} = P\Delta\widehat{Ptube}_{srow,sRet} + P\Delta\widehat{Phead}_{srow,sRet}$.

Flow velocities bounds:

$$yrow_{srow} = 0 \text{ for } srow \in (Svsminout \cup Svsmaxout) \tag{140}$$

$$yrow_{srow} = 0 \text{ for } srow \in (Svtminout \cup Svtmaxout) \tag{141}$$

where the sets *Svsminout*, *Svsmaxout*, *Svtminout*, and *Svtmaxout* are given by:

$$Svsminout = \left\{ srow / \widehat{Pvs}_{srow} \le \widehat{vsmin} - \hat{\varepsilon} \right\} \tag{142}$$

$$Svsmaxout = \left\{ srow / \widehat{Pvs}_{srow} \ge \widehat{vsmax} + \hat{\varepsilon} \right\} \tag{143}$$

$$Svtminout = \left\{ srow / \widehat{Pvt}_{srow} \le \widehat{vtmin} - \hat{\varepsilon} \right\} \tag{144}$$

$$Svtmaxout = \left\{ srow / \widehat{Pvt}_{srow} \ge \widehat{vtmax} + \hat{\varepsilon} \right\} \tag{145}$$

where $\hat{\varepsilon}$ is a small positive number.

4.6 | Geometric constraints

The same approach described above is applied to the geometric constraints, as follows:

Baffle spacing:

$$yrow_{srow} = 0 \text{ for } srow \in (SLNbminout \cup SLNbmaxout) \tag{146}$$

where the sets *SLNbminout* and *SLNbmaxout* are given by:

$$SLNbminout = \left\{ srow / \widehat{Plbc}_{srow} \le 0.2\widehat{PDs}_{srow} - \hat{\varepsilon} \right\} \quad (147)$$

$$SLNbmaxout = \left\{ srow / \widehat{Plbc}_{srow} \ge 1.0\widehat{PDs}_{srow} + \hat{\varepsilon} \right\} \quad (148)$$

The constraint related to *lbcmax* is:

$$\sum_{srow} \left(\widehat{Plbc}_{srow} \right) yrow_{srow} \le 0.5 \sum_{srow} \left(\widehat{plbmax1}\, \widehat{Pdte}_{srow} + \widehat{plbmax2} \right) yrow_{srow} \quad (149)$$

Tube length/shell diameter ratio:

$$yrow_{srow} = 0 \text{ for } srow \in (SLDminout \cup SLDmaxout) \quad (150)$$

where the sets *SLDminout* and *SLDmaxout* are given by:

$$SLDminout = \left\{ srow / \widehat{PL}_{srow} \le 3\widehat{PDs}_{srow} - \hat{\varepsilon} \right\} \quad (151)$$

$$SLDmaxout = \left\{ srow / \widehat{PL}_{srow} \ge 15\widehat{PDs}_{srow} + \hat{\varepsilon} \right\} \quad (152)$$

4.7 | Objective function

The heat transfer area when reformulated into the linear model is given by:

$$\text{Min } \pi \sum_{srow} \widehat{PNtt}_{srow} \widehat{Pdte}_{srow} \widehat{PL}_{srow} yrow_{srow} \quad (153)$$

The corresponding linear form of the total annualized cost is given by:

$$\begin{aligned} \text{Min } & \widehat{acost} \sum_{srow} \left(\pi \widehat{PNtt}_{srow} \widehat{Pdte}_{srow} \widehat{PL}_{srow} \right)^{\widehat{bcost}} yrow_{srow} \\ & + \widehat{ccost} \sum_{srow,sRet} \frac{\widehat{P\Delta Pt}_{srow,sRet} \widehat{mt}}{\widehat{\rho t}} wyrowRet_{srow,sRet} \\ & + \widehat{ccost} \sum_{srow,sRes} \frac{\widehat{P\Delta Ps}_{srow,sRes} \widehat{ms}}{\widehat{\rho s}} wyrowRes_{srow,sRes} \end{aligned} \quad (154)$$

5 | MODEL VALIDATION

The MILP model presented above was implemented in the GAMS software using the solver CPLEX. The example described and solved by Taborek[27] (section B of chapter 3.3.9) was used to validate this MILP model by fixing the geometric choices and then comparing different results. We fix the carrying error effect of rounding in the example by using larger number of significant figures. Results differ lower than 0.012% (corresponding to *Sb*), as shown in Table 1.

6 | COMPARISON WITH RESULTS FROM THE LITERATURE

Example 1, originally proposed by Shenoy,[31] is based on the minimization of heat transfer area, and Example 2, originally presented by Mizutani et al.,[16] involves the minimization of the total annualized cost. Both examples were solved by Ravagnani and Caballero[17] and Onishi et al.[18] using an MINLP formulation. The comparison of our results and Ravagnani and Caballero[17] and Onishi et al.[18] must consider some differences:

- The tube-side correlations in our model are different from the correlations used by Ravagnani and Caballero[17] and Onishi et al.[18] Our model for the evaluation of the tube-side convective heat transfer coefficient encompasses all flow regimes. In particular, in the turbulent regime, we use the Gnielinski correlation, but Ravagnani and Caballero[17] as well as Onishi et al.,[18] limited their analysis to turbulent flow and employed the Sieder and Tate correlation. According to Incropera and De Witt,[29] the Sieder and Tate correlation may yield errors up to 25%, while the errors of the Gnielinski correlation are lower than 10%;
- There are some differences between the equations used by Ravagnani and Caballero[17] and Onishi et al.[18] and the equations used by Taborek[27];
- Ravagnani and Caballero[17] and Onishi et al.[18] used baffle spacing as a variable, while we use the number of baffles as an integer variable. As a result, they obtain a spacing that leads to a noninteger number of baffles, which they round up to the nearest integer afterwards. They also include tube thickness as an optimization variable, but in our approach the tube thickness is defined by the user prior to the optimization;
- Ravagnani and Caballero[17] and Onishi et al.[18] formulations are nonconvex MINLP problems and they use a local solver that does not guarantee global optimality. Instead, our linear formulation guarantees the identification of the global optimum.

We compare the results from the original references of the corresponding examples,[16,31] with the solutions found by Ravagnani and Caballero[17] and Onishi et al.[18] and two sets of results generated with our model. The first set of our results corresponds to the rating of the previous solutions using our model and the second set contains the optimization results obtained using our MILP formulation. Table 2 describes the search space. All the results were generated considering tube-side velocities between 1 and 3 m/s and shell-side velocities between 0.5 and 2 m/s. All elapsed times reported here associated to the optimization runs were measured using a computer with a processor Intel Core i7 3.41 GHz with 16.6 GB RAM memory.

6.1 | Example 1

This problem was first presented by Shenoy.[31] The data of the problem streams are presented in Table 3. The thermal conductivity

TABLE 1 Validation results

Variable	Handbook	Our revision	Our numerical model	Deviation (%)
hi (W/m^2 °C)	2,133.50	2,130.6418	2,130.6418	0
hs (W/m^2 °C)	1,252.00	1,249.3178	1,249.3178	0
ΔPc (kPa)	3.90	3.9173	3.9173	0.0011
ΔPw (kPa)	6.40	6.3726	6.3727	0.0007
ΔPe (kPa)	3.40	3.5014	3.5014	0.0011
ΔPs (kPa)	13.70	13.7915	13.7915	0.0009

of the tube material is 50 W/m°C, both fouling resistances are 0.00015 m^2°C/W, and the available pressure drops are 42 and 7 kPa for the cold and hot streams, respectively. The minimum excess area is 0%. The allocation of the streams and the determination of the tube thickness are not variables in our optimization procedure, so we employed the values reported in the Ravagnani and Caballero solution[17]: the cold stream flows in the tube-side and the tube thickness is 1.225 mm. The rating of the results of Shenoy[31] and Caballero and Ravagnani[17] employed the reported values of shell-bundle clearances: 33 mm and 44 mm, respectively, but in the optimization using our model, this dimension was modeled according to Equation (30). The other clearances were determined according to Equations (31) and (35).

The comparison of the results is displayed in Table 4. The most relevant deviations in the rating of the literature solutions are for the pressure drops in the shell-side in relation to Ravagnani and Caballero[17] and the pressure drop in the tube-side in relation to Shenoy.[31] The optimal solution of our model, using a fixed baffle cut ratio equal to the previous references (0.25), has an area 16.8% lower than Shenoy[31] and 38.6.1% lower than Ravagnani and Caballero.[17] When including the baffle cut ratio in the optimization, the same value fixed in the previous reference was obtained. The elapsed time of the optimization using our model was 24 min. However, when the same problem was solved using a fixed baffle cut ratio the computational time was reduced to 4.1 min.

TABLE 2 Standard values of the discrete design variables

Variable	Values
Outer tube diameter, $\widehat{pdte}_{sd}$ (m)	0.01590, 0.01905, 0.02540
Tube length, $\widehat{pL}_{sL}$ (m)	2.438, 3.658, 4.877, 6.096, 6.706
Number of baffles, $\widehat{pNb}_{sNb}$	7, 8, ..., 25
Number of tube passes, $\widehat{pNpt}_{sNpt}$	1, 2, 4, 6, 8
Tube pitch ratio, $\widehat{prp}_{srp}$	1.25, 1.33, 1.50
Shell diameter, $\widehat{pDs}_{sDs}$ (m)	0.2050, 0.3048, 0.3366, 0.3874, 0.4382, 0.4890, 0.5398, 0.5906, 0.6350, 0.6858, 0.7366, 0.7874, 0.8382, 0.8890, 0.9398, 0.9906, 1.0668, 1.1430, 1.2192, 1.3716, 1.5240
Tube layout, $\widehat{play}_{slay}$	1 = triangular 30°, 2 = square 90°
Baffle cut ratio, $\widehat{pBc}_{sBc}$	0.20, 0.25, 0.30

The same problem was also solved by Onishi et al.,[18] using available pressure drops of 45 kPa for the cold stream and 10 kPa for the hot stream. Table 4 contains the solution reported by Onishi et al.,[18] the rating of this solution using our model with a shell bundle clearance of 31 mm, and the optimal solution found by our MILP formulation. Our solution obtained an optimal baffle cut ratio of 0.20 and rendered a reduction of the objective function equal to 19.91% with respect to that of Onishi et al.,[18] as shown in Table 4. The computational time to solve this problem was 22 min. If the baffle cut is fixed to 0.25, as it was adopted in Onishi et al.,[18] the reduction of the objective function is the same, but the computational time is reduced to 3.9 min.

We conclude that the differences in results are for the most part due to the fact that all previous works find local solutions whereas our is a global one. The differences do not stem from the usage of different correlations.

6.2 | Example 2

This problem was first presented by Mizutani et al.[16] The data of the problem streams are presented in Table 5. The thermal conductivity of the tube material is 50 W/m°C, the fouling resistance of both streams is 0.00017 m^2°C/W, and the maximum pressure drops are 68.95 kPa for both fluids. The minimum excess area is 0%. The economic parameters of the objective function are $\widehat{a_{cost}}$ = 123, $\widehat{b_{cost}}$ = 0.59, and $\widehat{c_{cost}}$ = 1.31. The allocation of the streams assumes that the cold stream flows in the tube-side and the tube thickness is equal to 1.675 mm. The rating of the results of Mizutani et al.,[16] Caballero and Ravagnani,[17] and Onishi et al.[18] employed the reported values of shell-bundle clearances: 15 mm, 42 mm, and 41 mm, respectively, but in the optimization this dimension was calculated accordingly.

Table 6 presents the results. The costs found by Mizutani et al.,[16] Ravagnani and Caballero,[17] and Onishi et al.[18] are similar, but the tradeoff between capital and operating costs is considerably different in each case: the capital cost found by Mizutani et al.[16] corresponds to 53.8% of the total cost, while Ravagnani and Caballero[17] found it is 70.5%. The total annualized cost of Onishi et al.[18] is slightly smaller than Mizutani et al.[16] and Ravagnani and Caballero.[17] The rating of the solution found by Ravagnani and Caballero[17] using our model yielded similar results. The differences in relation to the pressure

TABLE 3 Example 1—streams data

Stream	$\hat{m}$ (kg/s)	Inlet $\hat{T}$ (°C)	Outlet $\hat{T}$ (°C)	$\hat{\rho}$ (kg/m^3)	$\hat{\mu}$ (mPa·s)	$\widehat{Cp}$ (J/kg°C)	$\hat{k}$ (W/m°C)
Hot	14.90	98.0	65.0	777	0.23	2,684	0.11
Cold	31.58	15.0	25.0	998	1.00	4,180	0.60

TABLE 4 Example 1—results comparison—Ravagnani and Caballero[17]

Variable	Shenoy's[31] solution	Shenoy[31] rating using our model	Ravagnani and Caballero's[17] solution	Ravagnani and Caballero[17] rating using our model	Our MILP model original available pressure drops	Onishi et al.[18] solution	Onishi et al.[18] rating using our model	Our MILP model higher available pressure drops
Area (m^2)	28.40	28.40	38.52	38.52	23.64	28.89	28.90	23.14
dte (m)	0.01910	0.01910	0.01905	0.01905	0.01905	0.01905	0.01905	0.01590
dti (m)	0.01540	0.01540	0.01660	0.01660	0.01660	0.01660	0.01660	0.01345
Ds (m)	0.549	0.549	0.533	0.533	0.387	0.387	0.387	0.387
lay	Square	Square	Square	Square	Square	Square	Square	Triangular
Npt	6	6	2	2	2	2	2	2
rp	1.33	1.33	1.33	1.33	1.25	1.33	1.33	1.50
L (m)	1.286	1.286	2.438	2.438	2.438	3.658	3.658	2.438
Nb	6	6	19	19	7	9	9	9
Ntt	368	368	264	264	162	132	132	190
vt (m/s)	-	2.770	1.108	1.108	1.805	2.215	2.215	2.344
vs (m/s)	-	0.668	1.162	0.980	0.737	0.517	0.457	0.589
ht (W/m^2°C)	8,649.6	10,145.8	4,087.1	5,484.6	8,506.8	7,283.9	10,216.3	10,989.2
hs (W/m^2°C)	1,364.5	1,321.4	1,308.4	1,418.4	1,700.3	2,096.0	1,249.0	1,762.8
ΔPt (kPa)	42.000	86.637	7.706	7.551	18.540	43.040	36.738	36.249
ΔPs (kPa)	3.600	3.195	7.000	10.434	6.491	10.000	4.233	8.856

Abbreviation: MILP, mixed-integer linear programming problem.

drops and heat transfer coefficients are not higher than 10%. The solution of Onishi et al.[18] and Mizutani et al.[16] showed maximum deviations of 20%, except the shell-side pressure drop. The optimal solutions of Mizutani et al.,[16] Ravagnani and Caballero,[17] and Onishi et al.[18] are based on a fixed baffle cut ratio of 0.25 and the inclusion of this parameter as a variable in our model yielded an optimal baffle cut ratio of 0.30. The elapsed time of the optimization was 48 min.

Our MILP solution presents a total annualized cost that is considerably lower when compared to the results of Mizutani et al.,[16] Ravagnani and Caballero,[17] and Onishi et al.[18] When comparing our solution to the other cited works, we find that the main reason for this large cost reduction is the decrease of the total number of tube passes to 1, which allowed a reduction of the pumping costs, through the decrease of the total length of the hydraulic path, and an increase of the mean temperature difference (the correction factor for the multipass configuration is 0.812 and is increased to 1 in the countercurrent configuration).

As in Example 1, we believe the large differences in results are mostly due to the fact that the solutions obtained in previous work are local solutions. As we checked the issue, we think that they are not attributable to the differences in correlations and/or modeling.

7 | COMPARISON WITH RESULTS USING THE KERN METHOD

Table 7 displays a comparison of the application of the proposed approach with the results present in Gonçalves et al.[20] for 10 heat exchanger design problems. Both approaches are based on linear formulations; in our case, we used the Bell–Delaware method, and in the case of Gonçalves et al.,[20] the Kern method was employed.

The heat transfer areas calculated using the Kern method are on average 22% higher than the corresponding results using the Bell–Delaware

TABLE 5 Example 2—streams data

Stream	$\hat{m}$ (kg/s)	Inlet $\hat{T}$ (°C)	Outlet $\hat{T}$ (°C)	$\hat{\rho}$ (kg/m^3)	$\hat{\mu}$ (mPa·s)	$\widehat{cp}$ (J/kg°C)	$\hat{k}$ (W/m°C)
Hot	27.78	95.0	40.0	750	0.34	2,840	0.19
Cold	68.88	25.0	40.0	995	0.80	4,200	0.59

TABLE 6 Example 2—results comparison

Variable	Mizutani et al.'s[16] solution	Mizutani et al.[16] rating using our model	Ravagnani and Caballero's[17] solution	Ravagnani and Caballero[17] rating using our model	Onishi et al.[18] solution	Onishi et al.[18] rating using our model	Our MILP model
Total cost ($/y)	5,250.00	5,279.56	5,191.47	5,137.78	5,134.21	4,853.40	3,754.01
Area cost ($/y)	2,826.00	2,825.45	3,663.23	3,461.77	3,175.61	3,175.61	2,510.14
Pumping cost ($/y)	2,424.00	2,454.11	1,528.24	1,676.02	1,958.59	1,677.79	1,243.86
Area (m^2)	202.00	202.81	286.15	286.15	247.22	247.22	165.95
dte (m)	0.01590	0.01590	0.01905	0.01905	0.01905	0.01905	0.01590
dti (m)	0.01260	0.01260	0.01570	0.01570	0.01660	0.01660	0.01255
Ds (m)	0.687	0.687	0.838	0.838	0.787	0.787	0.591
lay	Square	Square	Square	Square	Square	Square	Square
Npt	2	2	2	2	2	2	1
rp	1.25	1.25	1.33	1.33	1.33	1.33	1.33
L (m)	4.877	4.877	6.706	6.706	6.706	6.706	6.096
Nb	8	8	18	18	17	17	12
Ntt	832	832	713	713	616	616	545
vt (m/s)	-	1.334	1.003	1.003	1.039	1.039	1.027
vs (m/s)	-	0.467	0.500	0.447	0.500	0.449	0.512
ht ($W/m^{2\circ}C$)	6,480.0	7,400.0	4,186.2	5,599.4	4,356.7	5,743.4	5,846.7
hs ($W/m^{2\circ}C$)	1,829.0	1,951.7	1,516.5	1,558.8	1,880.2	1,591.6	1,972.0
ΔPt (kPa)	22.676	23.553	13.404	14.701	15.921	14.729	8.650
ΔPs (kPa)	7.494	6.558	6.445	7.065	10.609	7.049	9.468

Abbreviation: MILP, mixed-integer linear programming problem.

TABLE 7 Kern method and Bell method—results comparison

Example	Kern method		Bell method	
	Heat transfer area (m^2)	Elapsed time (s)	Heat transfer area (m^2)	Elapsed time (s)
1	624	12	524	232
2	319	11	274	271
3	199	11	158	134
4	872	12	712	146
5	144	12	123	136
6	332	11	284	251
7	207	12	171	164
8	914	12	841	211
9	287	12	219	341
10	327	12	238	118

method. Due to the higher complexity of the model, the computational times employed by the Bell–Delaware method are higher than those used to solve the optimization design problems with the Kern method.

8 | CONCLUSIONS

By recognizing that the geometric variables have discrete representations, we rigorously reformulated the entire MINLP problem of the design optimization of shell-and-tube heat exchangers using the Bell–Delaware method in a form of an MILP problem. Our reformulation is not an approximation or a linearization by truncating Taylor series. Rather, it is rigorous, in the sense that the feasible solutions of the MINLP model are also feasible in the MILP model and vice-versa. We validated our implemented approach through its comparison with a literature result.[27] The proposed approach can identify solutions that are significantly better, the most relevant reason for the significant improvement is the local nature of the optimum found by other approaches.

ACKNOWLEDGMENTS

André L. H. Costa thanks the National Council for Scientific and Technological Development (CNPq) for the research productivity fellowship (Process 311225/2016-0) and the financial support of the Prociência Program (UERJ). Caroline de O. Gonçalves thanks the Carlos Chagas Filho Research Support Foundation (FAPERJ) for the scholarship.

NOTATION

Sets

sBc	baffe cut, 1, ..., *sBcmax*
sd	tube diameter, 1, ..., *sdmax*
sDs	shell diameter, 1, ..., *sDsmax*

sL	tube length, 1, ..., *sLmax*
slay	tube layout, 1, ..., *slaymax*
sNb	number of baffles, 1, ..., *sNbmax*
sNpt	number of tube passes, 1, ..., *sNptmax*
srp	tube pitch ratio, 1, ..., *srpmax*
srow	multi-index
sNut	number of Nusselt, 1, ..., *sNutmax*
sRes	number of Reynolds on shell-side, 1, ..., *sResmax*

Parameters

$\widehat{acost}$	area cost constant
$\widehat{Aexc}$	excess area, %
$\widehat{bcost}$	area cost constant
$\widehat{ccost}$	pumping cost constant
$\widehat{cp}$	heat capacity, J/kg K
$\hat{F}_{srow}$	correction factor to logarithmic mean temperature difference
$\hat{k}$	thermal conductivity, W/m K
$\hat{m}$	mass flow rate, kg/s
$\hat{P}$	LMTD correction factor parameter
$\widehat{PBc}_{srow}$	baffle cut, %
$\widehat{PDs}_{srow}$	shell diameter, m
$\widehat{Pdte}_{srow}$	outer tube diameter, m
$\widehat{Pdti}_{srow}$	inner tube diameter, m
$\widehat{PL}_{srow}$	tube length, m
$\widehat{Play}_{srow}$	tube layout
$\widehat{pLtb}_{sDs,sL,sNb}$	diametral clearance between the outer tube diameter and the baffle hole
$\widehat{PNb}_{srow}$	number of baffles
$\widehat{PNpt}_{srow}$	number of tube passes
$\widehat{PNtt}_{srow}$	total number of tubes
$\widehat{Pr}$	Prandtl number
$\widehat{Prp}_{srow}$	tube pitch ratio
$\hat{Q}$	heat duty, W
$\hat{R}$	LMTD correction factor parameter
$\widehat{Rf}$	fouling factor, m^2 K/W
$\hat{T}$	temperature, °C
$\widehat{UNut}$	upper bound on the Nusselt number
$\widehat{URet}$	upper bond on the Reynolds number
$\hat{\rho}$	density, kg/m^3
$\hat{\mu}$	viscosity, Pa·s
$\Delta\widehat{Pdisp}$	available pressure drop, Pa
$\Delta\widehat{Tlm}$	log-mean temperature difference
$\widehat{P\psi}_{nsNpt,sDs}$	correction factor of the omission of tubes inside the shell due to the presence of multiple tube passes
$\hat{\varepsilon}$	small positive number

Binary variables

yBc_{sBc}	variable representing the baffle cut
yd_{sd}	variable representing the tube diameter
yDs_{sDs}	variable representing the shell diameter
yL_{sL}	variable representing the tube length
$ylay_{slay}$	variable representing the tube layout
yNb_{sNb}	variable representing the number of baffles
$yNpt_{sNpt}$	variable representing the number of tube passes
yrp_{srp}	variable representing the tube pitch ratio
$yrow_{srow}$	variable representing the set of variables
$yRet_{sRet}$	variable representing the Reynolds number on tube-side
$yRes_{sRes}$	variable representing the Reynolds number on shell-side
$yNut_{sNut}$	variable representing the Nusselt number

Continuous variables

A	heat exchange area, m^2
a, *a*1, *a*2, *a*3, *a*4	empirical coefficients
b, *b1*, *b2*, *b3*, *b4*	empirical coefficients
Bc	baffle cut
d	tube diameter, m
Dctl	diameter of the circle delimited by the centers of the outer tubes of the bundle, m
Dotl	tube bundle circumscribed circle diameter, m
Ds	shell diameter, m
Dw	equivalent hydraulic diameter of a segmental baffle window, m
f	friction factor
Fc	fraction of total tubes in cross-flow
Fsbp	fraction of cross-flow area available for bypass flow
Fw	fraction of number of tubes in one windows
Gs	mass flux, kg/m^2
h	convective heat transfer coefficient, W/m^2 K
hi	shell-side heat transfer coefficient for an ideal tube bank, W/m^2 K
Jb	correction factor for bundle-bypassing effects
Jc	correction factor for baffle configuration effects
ji	Colburn factor
Jl	correction factor for baffle-leakage effects
Jr	the laminar heat transfer correction factor
L	tube length, m
lay	tube layout
Lbb	diametral clearance between the shell and the tube bundle, m
lbc	baffle spacing, m
Lpl	length which expresses the effect of the tube lane partition bypass width, m
Lsb	shell-to-baffle diametral clearance, m
Ltb	diametral clearance between tube outside diameter and baffle hole, m

ltp	tube pitch, m
Nb	number of baffles
Nc	total number of rows crossed along the entire heat exchanger
Npt	number of tube passes
Ntcc	number of tube rows crossed in one cross-flow section
Ntcw	number of tube columns effectively crossed in each window
Ntp	number of tubes per passes
Ntt	total number of tubes
Ntw	number of tubes in the window
Nu	Nusselt number
Rb	pressure drop correction factor for bundle-bypassing effects
Re	Reynolds number
Rl	pressure drop correction factor for baffle-leakage effects, Pa
rp	tube pitch ratio
rs	ratio of the shell-to-baffle leakage area to the sum of both leakage area
Rs	pressure drop correction for unequal baffle spacing at inlet and or outlet
rlm	ratio of both leakage areas to the cross-flow area
Sb	bypass area within one baffle, m^2
Sm	reference normal area for shell-side flow, m^2
Ssb	shell-to-baffle leakage area, m^2
Stb	tube-to-baffle clearance, m
Sw	area flow thought the window, m^2
Swg	gross window area, m^2
Swt	window area occupied by tubes, m^2
U	overall heat transfer coefficient, W/m^2 K
v	velocity, m/s
ΔP	pressure drop, Pa
ΔPbi	shell-side pressure drop for ideal cross-flow, Pa
ΔPc	pressure drop in pure cross flow, Pa
ΔPe	pressure drop in the end zones, Pa
ΔPw	pressure drop in the baffle window, Pa
ψ_n	correction factor of the omission of tubes inside the shell due to the presence of multiple tube passes
θctl	central angle delimited by the intercession between the baffle cut edge and the circle associated to the centers of the outer tubes
θDs	central angle defined by the intercession of the baffle cut edge with the shell

ORCID

André L. H. Costa https://orcid.org/0000-0001-9167-8754
Miguel J. Bagajewicz https://orcid.org/0000-0003-2195-0833

REFERENCES

1. Saunders EAD. *Heat Exchangers: Selection, Design and Construction*. New York, NY: John Wiley & Sons; 1988.
2. Jegede FO, Polley GT. Optimum heat exchanger design. *Chem Eng Res Des*. 1992;70(A2):133-141.
3. Tharakeshwar TK, Seetharamu KN, Durga Prasad B. Multi-objective optimization using bat algorithm for shell and tube heat exchangers. *Appl Therm Eng*. 2017;110:1029-1038.
4. Muralikrishna K, Shenoy UV. Heat exchanger design targets for minimum area and cost. *Trans IChemE*. 2000;78(Part A):161-167.
5. Ravagnani MASS, Silva AP, Andrade AL. Detailed equipment design in heat exchanger networks synthesis and optimization. *Appl Therm Eng*. 2003;23:141-151.
6. Chaudhuri PD, Diwekar UM. An automated approach for the optimal design of heat exchangers. *Ind Eng Chem Res*. 1997;36:3685-3693.
7. Ponce-Ortega JM, Serna-González M, Jiménez-Gutiérrez A. Use of genetic algorithms for the optimal design of shell-and-tube heat exchangers. *Appl Therm Eng*. 2009;29:203-209.
8. Yang J, Fan A, Liu W. Optimization of shell-and-tube heat exchangers conforming to TEMA standards with designs motivated by constructal theory. *Energ Conver Manage*. 2013;78:468-476.
9. Ravagnani MASS, Silva AP, Biscaia EC, Caballero JA. Optimal design of shell-and-tube heat exchangers using particle swarm optimization. *Ind Eng Chem*. 2009;48:2927-2935.
10. Şahin AŞ, Kılıç B, Kılıç U. Design and economic optimization of shell and tube heat exchangers using Artificial Bee Colony (ABC) algorithm. *Energ Conver Manage*. 2011;52:3356-3362.
11. Mohanty DK. Application of firefly algorithm for design optimization of a shell and tube heat exchanger from economic point of view. *Int J Therm Sci*. 2016;102:228-238.
12. Khosravi R, Khosravi A, Nahavandi S, Hajabdollahi H. Effectiveness of evolutionary algorithms for optimization of heat exchangers. *Energ Conver Manage*. 2015;89:281-288.
13. Sadeghzadeh H, Ehyaei MA, Rosen MA. Techno-economic optimization of a shell and tube heat exchanger by genetic and particle swarm algorithms. *Energ Conver Manage*. 2015;93:84-91.
14. Saldanha WH, Soares GL, Machado-Coelho TM, Dos Santos ED, Ekel PI. Choosing the best evolutionary algorithm to optimize the multiobjective shell-and-tube heat exchanger design problem using PROMETHEE. *Appl Therm Eng*. 2017;127:1049-1061.
15. Aras O, Bayramoğlu M. A MINLP study on shell and tube heat exchanger: hybrid branch and bound/meta-heuristics approaches. *I&EC Res*. 2012;51:14158-14170.
16. Mizutani FT, Pessoa FLP, Queiroz EM, Hauan S, Grossmann IE. Mathematical programming model for heat-exchanger network synthesis including detailed heat-exchanger designs. *Ind Eng Chem Res*. 2003;42:4009-4018.
17. Ravagnani MASS, Caballero JA. A MINLP model for the rigorous design of shell and tube heat exchangers using the TEMA standards. *Chem Eng Res Des*. 2007;85:1423-1435.
18. Onishi VC, Ravagnani MASS, Caballero JA. Mathematical programming model for heat exchanger design through optimization of partial objectives. *Energ Conver Manage*. 2013;74:60-69.
19. Gonçalves CO, Costa ALH, Bagajewicz MJ. Shell and tube heat exchanger design using mixed-integer linear programming. *AIChE J*. 2017;63(6):1907-1922.
20. Gonçalves CO, Costa ALH, Bagajewicz MJ. Alternative MILP formulation for shell and tube heat exchanger optimal design. *Ind Eng Chem Res*. 2017;56(20):5970-5979.
21. Towler G, Sinnot R. *Chemical Engineering Design – Principles, Practice and Economics of Plant And Process Design*. Burlington, NJ: Butterworth-Heinemann; 2008.
22. Serth RW. *Process Heat Transfer: Principles and Applications*. Amsterdam: Elsevier; 2007.

23. Kern DQ. *Process Heat Transfer*. New York, NY: McGraw-Hill; 1950.
24. Bell KJ. Logic of the design process. In: Hewitt GF, ed. *Heat Exchanger Design Handbook*. New York, NJ: Begell House; 1960.
25. Schilling RL, Bell KJ, Bernhagen PM, et al. Heat-transfer equipment. In: Perry RH, Green DW, Maloney JO, eds. *Perry's Chemical Engineers' Handbook*. New York, NY: McGraw-Hill; 1999.
26. Ludwig E. *Applied Process Design for Chemical and Petrochemical Plants*. 3rd ed. Oxford, UK: Gulf Professional Publishing; 2001.
27. Taborek J. Input data and recommended practices. In: Hewitt GF, ed. *Heat Exchanger Design Handbook*. New York, NY: Begell House; 2008.
28. TEMA. *Standards of the Tubular Exchangers Manufactures Association*. 9th ed. New York: Tubular Exchanger Manufacturers Association; 2007.
29. Incropera FP, De Witt DP. *Fundamentals of Heat and Mass Transfer*. 6th ed. Hoboken: John Wiley & Sons; 2006.
30. Souza P, Costa ALH, Bagajewicz MJ. Globally optimal linear approach for the design of process equipment: the case of air coolers. *AIChE J*. 2017;64:886-903. https://doi.org/10.1002/aic.15977.
31. Shenoy UV. *Heat Exchanger Network Synthesis – Process Optimization by Energy And Resource Analysis*. Houston: Gulf Publishing Company; 1995.

SUPPORTING INFORMATION

Additional supporting information may be found online in the Supporting Information section at the end of this article.

How to cite this article: Gonçalves Caroline de O., Costa ALH, Bagajewicz MJ. Linear method for the design of shell and tube heat exchangers using the Bell–Delaware method. *AIChE J*. 2019;65:e16602. https://doi.org/10.1002/aic.16602